

Fig. 4. Total attenuation of a shielded 75Ω microstrip line versus frequency with surface roughness parameter of σ_{eff} at the interfaces between conductor and substrate. Dimensions of substrate and microstrip: $w = 130 \mu\text{m}$, $h = 200 \mu\text{m}$, $t = 35 \mu\text{m}$, $\kappa = 58 \cdot 10^6 [\Omega\text{m}]^{-1}$, and $\epsilon_r = 5$. Metallic shielding: $1235 \times 1640 \mu\text{m}^2$.

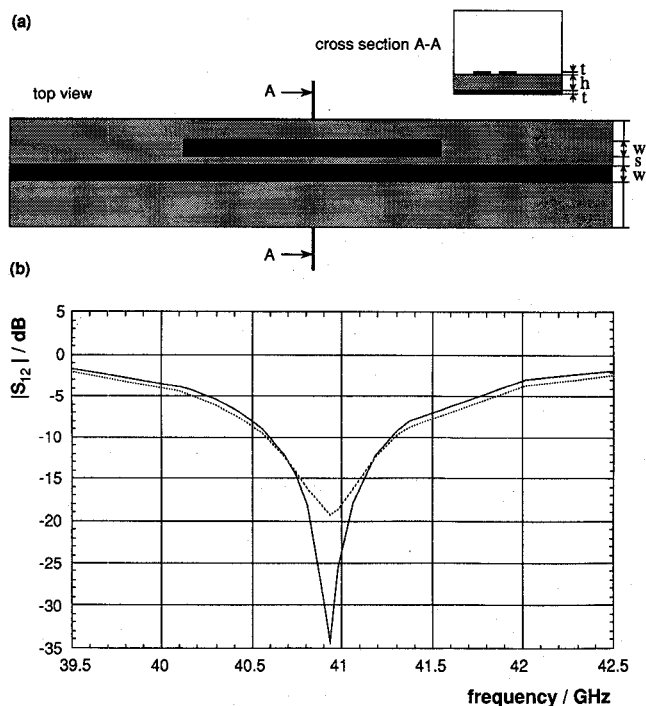


Fig. 5. Configuration (a), and magnitude of the transmission coefficient S_{12} (b), for a microstrip parallel resonator (one wavelength long at resonance), showing the influence of copper metallization and conductor roughness. $w = 150 \mu\text{m}$, $h = 150 \mu\text{m}$, $t = 30 \mu\text{m}$, $s = 75 \mu\text{m}$, $\kappa = 58 \cdot 10^6 [\Omega\text{m}]^{-1}$ and $\epsilon_r = 12.9$ copper $\sigma_{\text{eff}} = 0.25 \mu\text{m}$. — ideal conductor.

compared to a real copper conductor with a finite surface roughness. The resonator quality factor is lowered as expected by the conductor losses.

V. CONCLUSIONS

An extension of the finite difference method in frequency domain for accurate and effective treatment of conductor losses and surface

roughness was presented. The results confirm that the approach is applicable as long as the conditions for the skin depth are fulfilled. The introduction of discretization cells with a surface resistance reduces the total number of required cells by use of a frequency independent coarse grid. The method has the advantage of giving only a small decrease of convergence stability compared to the lossless calculation.

The proposed method is well suited for CAD.

ACKNOWLEDGMENT

The authors would like to thank Dr. Heinrich of the Ferdinand and Braun Institute Berlin for performing reference calculations with the mode matching method to check the presented method versus his results.

REFERENCES

- [1] S. Haffa, D. Hollmann, and W. Wiesbeck, "The finite difference method for S -parameter calculation of arbitrary three-dimensional structures," *IEEE Trans. Microwave Theory Tech.*, vol. 40, pp. 1602-1610, Aug. 1992.
- [2] A. Christ and H. Hartnagel, "Three-dimensional finite-difference method for the analysis of microwave-device embedding," *IEEE Trans. Microwave Theory Tech.*, vol. MTT-35, pp. 688-696, Aug. 1987.
- [3] D. Hollmann, S. Haffa, and W. Wiesbeck, "Full wave analysis for S -parameter calculation of arbitrary three-dimensional lossy structures," in *Proc. 12th European Microwave Conf.*, Budapest, Sept. 1990, pp. 1065-1070.
- [4] K. S. Yee, "Numerical solution of initial boundary value problems involving Maxwell's equation in isotropic media," *IEEE Trans. Antennas Propagat.*, vol. AP-14, pp. 302-307, May 1966.
- [5] S. P. Morgan, "Effect of surface roughness on eddy current losses at microwave frequencies," *J. Appl. Phys.*, vol. 20, pp. 352-362, 1949.
- [6] R. K. Hoffmann, *Integrierte Mikrowellenschaltungen*, Berlin, Heidelberg, New York: Springer Verlag, 1983, pp. 201-203.
- [7] W. Heinrich, "Full-wave analysis of conductor losses on MMIC transmission lines," *IEEE Trans. Microwave Theory Tech.*, vol. 38, pp. 1468-1472, Oct. 1990.

TM-Scattering from a Slit in a Thick Conducting Screen: Revisited

Soo H. Kang, Hyo J. Eom, and Tah J. Park

Abstract—TM plane-wave scattering from a slit in a thick conducting screen is reexamined. A Fourier transform technique is employed to express the scattered field in the spectral domain, and the boundary conditions are enforced to obtain simultaneous equations for the transmitted field inside the thick conducting screen. The simultaneous equations are solved to represent the transmitted and scattered fields in series forms. Approximate series solutions for scattering and transmission are obtained in closed-forms which are valid for high-frequency scattering regime.

Manuscript received April 2, 1992; revised September 10, 1992.

The authors are with the Department of Electrical Engineering, Korea Advanced Institute of Science and Technology, 373-1, Kusong Dong, Yusung Gu, Taejon, Korea.

IEEE Log Number 9207434.

I. INTRODUCTION

Electromagnetic scattering from a slit in a thick conducting screen has been extensively studied [1]–[6]; however, the exact solution is not available in a closed form, thus rendering to various approximations and numerical approaches to understand the behavior of scattering from and transmission through the slit.

In this paper, using the technique of Fourier transform and mode-matching given in [5], we obtain a solution for uniform plane wave scattering from a slit in the thick perfectly conducting screen. The solution presented in this paper is not only computationally efficient but also it reduces to a simple closed form under certain conditions.

The organization of the paper is as follows: In the next section, we show the expressions for the TM (transverse magnetic to slit axis) scattered wave which is represented in the spectral domain by using the boundary conditions. In Section III, we perform the numerical calculations for the transmitted field and the transmission coefficient to compare them with other existing solutions. A brief summary is given in the Conclusion.

II. FIELD REPRESENTATIONS AND MATCHING BOUNDARY CONDITIONS

A. Field Representations

In region (I) (air, $z > 0$), an incident field E_y^i impinges on a slit (width: $2a$, depth: d) in a thick perfectly conducting screen (See Fig. 1). Region (II) ($-d < z < 0, -a < x < a$) denotes the slit filled with a lossy material. Region (III) denotes the lossless half-space ($z < -d$). The wave number of regions (I), (II), and (III) are k_0 , k_1 , and k_2 , respectively. Note $k_0 = w\sqrt{\mu_0\epsilon_0}$, $k_1 = w\sqrt{\mu_1\epsilon_1}$, and $k_2 = w\sqrt{\mu_2\epsilon_2}$. Here, $\exp(-jwt)$ time-harmonic variation is suppressed throughout.

Then in region (I), the total electric field consists of the incident, the reflected, and the scattered fields which are respectively written as

$$\begin{aligned} E_y^i(x, z) &= e^{jk_x x - jk_z z} \\ E_y^r(x, z) &= -e^{jk_x x + jk_z z} \\ E_y^s(x, z) &= 1/(2\pi) \int_{-\infty}^{\infty} \tilde{E}_y^s(\zeta) e^{-j\zeta x + jk'_0 z} d\zeta \end{aligned}$$

where

$$\begin{aligned} k_x &= k_0 \sin \theta \\ k_z &= k_0 \cos \theta \\ k'_0 &= \sqrt{k_0^2 - \zeta^2} \\ \tilde{E}_y^s(\zeta) &= \int_{-\infty}^{\infty} E_y^s(x, 0) e^{j\zeta x} dx \end{aligned}$$

Note that $\tilde{E}_y^s(\zeta)$ and $E_y^s(x, 0)$ are the Fourier transform pair.

Since $H_x(x, z) = -1/(j\omega\mu_0)\partial E_y(x, z)/\partial z$, the corresponding x components of the incident, the reflected, and the scattered H -fields are

$$\begin{aligned} H_x^i(x, z) &= \frac{k_z}{\omega\mu_0} e^{jk_x x - jk_z z} \\ H_x^r(x, z) &= \frac{k_z}{\omega\mu_0} e^{jk_x x + jk_z z} \\ H_x^s(x, z) &= \frac{-1}{\omega\mu_0} \int_{-\infty}^{\infty} \frac{k'_0}{2\pi} \tilde{E}_y^s(\zeta) e^{-j\zeta x + jk'_0 z} d\zeta \end{aligned}$$

In region (II), the total field in between the screen may be represented as

$$E_y^d(x, z) = \sum_{m=1}^{\infty} (b_m \cos \xi_m z + c_m \sin \xi_m z) \sin a_m(x + a)$$

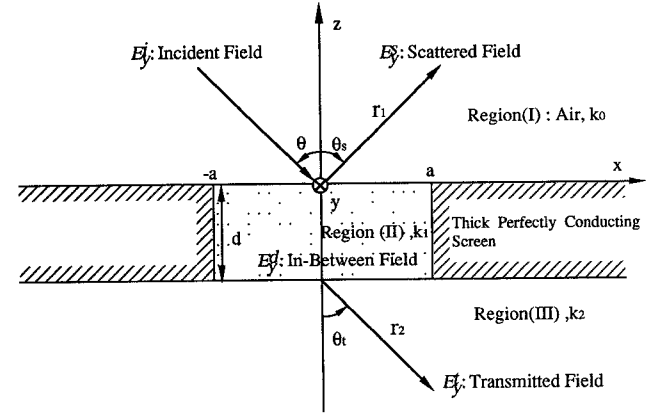


Fig. 1. Geometry of scattering from a thick perfectly conducting screen.

(2.1)

where

$$a_m = m\pi/(2a)$$

$$\xi_m = \sqrt{k_1^2 - a_m^2}$$

The corresponding x component of H -field is

$$H_x^d(x, z) = \frac{-1}{j\omega\mu_1} \sum_{m=1}^{\infty} \xi_m \cdot (-b_m \sin \xi_m z + c_m \cos \xi_m z) \sin a_m(x + a)$$

In region (III), the total transmitted field may be written as

$$E_y^t(x, z) = \frac{1}{2\pi} \int_{-\infty}^{\infty} \tilde{E}_y^t(\zeta) e^{-j\zeta x - jk'_2(z+d)} d\zeta$$

where

$$k'_2 = \sqrt{k_2^2 - \zeta^2}$$

$$\tilde{E}_y^t(\zeta) = \int_{-\infty}^{\infty} E_y^t(x, -d) e^{j\zeta x} dx$$

The corresponding x component of H -field is

$$H_x^t(x, z) = \frac{1}{\omega\mu_2} \int_{-\infty}^{\infty} \frac{k'_2}{2\pi} \tilde{E}_y^t(\zeta) e^{-j\zeta x - jk'_2(z+d)} d\zeta$$

B. Matching Boundary Conditions

To determine unknown coefficients b_m and c_m , it is necessary to match the boundary conditions of tangential E - and H -field continuities. First, the tangential E -field continuity along the x -axis ($-\infty < x < \infty, z = 0$) yields

$$\begin{aligned} E_y^s(x, 0) &= E_y^d(x, 0) \quad |x| < a \\ &= 0 \quad |x| > a \end{aligned}$$

Taking the Fourier transform on the both sides of above equation, we get

$$\begin{aligned} \tilde{E}_y^s(\zeta) &= \int_{-\infty}^{\infty} E_y^s(x, 0) e^{j\zeta x} dx \\ &= \int_{-a}^a E_y^d(x, 0) e^{j\zeta x} dx \end{aligned} \quad (2.2)$$

Substituting (2.1) into (2.2), and performing integration with respect to x , we obtain

$$\tilde{E}_y^s(\zeta) = \sum_{m=1}^{\infty} b_m \frac{a_m}{(\zeta^2 - a_m^2)} \cdot [e^{j\zeta a} (-1)^m - e^{-j\zeta a}] \quad (2.3)$$

Second, the tangential H -field continuity along $-a < x < a, z = 0$, gives

$$\begin{aligned} H_x^t(x, 0) + H_x^r(x, 0) + H_x^s(x, 0) &= H_x^d(x, 0) \\ \frac{2jk_z}{\mu_0} e^{jk_z x} - \int_{-\infty}^{\infty} \frac{jk'_0}{2\pi\mu_0} \tilde{E}_y^s(\zeta) e^{-j\zeta x} d\zeta \\ &= \sum_{m=1}^{\infty} -\frac{c_m \xi_m}{\mu_1} \sin a_m(x + a) \end{aligned} \quad (2.4)$$

Substituting (2.3) into (2.4), we obtain

$$\begin{aligned} \frac{2jk_z}{\mu_0} e^{jk_z x} - \frac{j}{2\pi\mu_0} \sum_{m=1}^{\infty} \\ b_m a_m \int_{-\infty}^{\infty} \frac{(-1)^m e^{j\zeta a} - e^{-j\zeta a}}{\zeta^2 - a_m^2} k'_0 e^{-j\zeta x} d\zeta \\ = \sum_{m=1}^{\infty} -\frac{c_m \xi_m}{\mu_1} \sin a_m(x + a) \end{aligned}$$

Multiplying the above equation by $\sin a_n(x + a)$ and integrating the both sides with respect to x from $-a$ to a , we obtain

$$\begin{aligned} \frac{2jk_z a_n}{\mu_0(a_n^2 - k_z^2)} [(-1)^n e^{jk_z a} + e^{-jk_z a}] \\ = \frac{ja_n}{2\pi\mu_0} \sum_{m=1}^{\infty} b_m a_m I(k_0) - \frac{c_n \xi_n a}{\mu_1} \end{aligned} \quad (2.5)$$

where

$$I(k_0) = \int_{-\infty}^{\infty} \frac{[(-1)^m e^{j\zeta a} - e^{-j\zeta a}] [(-1)^n e^{-j\zeta a} - e^{j\zeta a}] k'_0}{(\zeta^2 - a_m^2)(\zeta^2 - a_n^2)} d\zeta$$

Using the residue calculus, we may evaluate $I(k_0)$ as [7]

$$I(k_0) = \frac{2\pi a \eta_m}{a_m^2} \delta_{mn} - [I_1(k_0) + I_2(k_0)] \quad (2.6)$$

where δ_{mn} is the Kronecker delta, and $\eta_m = \sqrt{k_0^2 - a_m^2}$. The first term containing δ_{mn} is a residue contribution at $\zeta = \pm a_m$ whereas $I_1(k_0)$ and $I_2(k_0)$ arise from the integration along the branch cut associated with $\zeta = k_0$.

$$\begin{aligned} I_1(k_0) &= \int_{-0}^{\infty} \frac{-4j(-1)^n e^{2jk_0 a} e^{-2k_0 a v} \sqrt{v(-2j+v)}}{k_0^2[(1+jv)^2 - \alpha^2][(1+jv)^2 - \beta^2]} dv \quad (2.7) \\ &= -\frac{2e^{2jk_0 a}(-1)^n}{k_0^2(\alpha^2 - \beta^2)} \sum_{l=1}^{\infty} S_l \{ [A(t_1) - A(t_2)]/\alpha \\ &\quad - [A(t_3) - A(t_4)]/\beta \} \end{aligned} \quad (2.8)$$

$$I_2(k_0) = \frac{-4j}{k_0^2(\alpha^2 - \beta^2)} \left[-\frac{\sqrt{1 - \alpha^2}}{\alpha} \sin^{-1} \alpha + \frac{\sqrt{1 - \beta^2}}{\beta} \sin^{-1} \beta \right]$$

$$\alpha = a_m/k_0, \beta = a_n/k_0$$

$$A(t) = (-1)^l \pi t^{l-0.5} e^{pt} \operatorname{erfc}(\sqrt{pt}) + 2^{1-l} \sqrt{\pi} p^{0.5-l}$$

$$\cdot \sum_{r=0}^{l-1} (2l-2r-3)!! (-2pt)^r$$

$$p = 2k_0 a$$

$$t_1 = (\alpha - 1)j, t_2 = (-\alpha - 1)j$$

$$t_3 = (\beta - 1)j, t_4 = (-\beta - 1)j$$

$\operatorname{erfc}(\dots)$ complementary error function

The expression $I_1(k_0)$ in (2.8) is an asymptotic series form of which l th term has an order $O[1/(k_0 a)^{l-0.5}]$. Note that this asymptotic series expression converges for $|2k_0 a/(m\pi)| > 1$.

Hence, it is computationally more efficient to use (2.7) than (2.8) in evaluating $I_1(k_0)$.

In order to determine the coefficients b_m and c_m , we use another boundary condition at $z = -d$. The tangential E -field continuity along $z = -d$, gives

$$\begin{aligned} E_y^d(x, -d) &= E_y^t(x, -d) \quad |x| < a \\ &= 0 \quad |x| > a \end{aligned}$$

Taking the Fourier transform on the both sides of above equation, we get

$$\begin{aligned} \tilde{E}_y^t(\zeta) &= \sum_{m=1}^{\infty} (b_m \cos \xi_m d - c_m \sin \xi_m d) \\ &\quad \cdot \frac{a_m}{\zeta^2 - a_m^2} [e^{j\zeta a} (-1)^m - e^{-j\zeta a}] \end{aligned} \quad (2.9)$$

The tangential H -field continuity along $-a < x < a, z = -d$, gives

$$\begin{aligned} j \frac{\mu_2}{\mu_1} \sum_{m=1}^{\infty} (b_m \sin \xi_m d + c_m \cos \xi_m d) \xi_m \sin a_m(x + a) \\ = \int_{-\infty}^{\infty} \frac{k'_2}{2\pi} \tilde{E}_y^t(\zeta) e^{-j\zeta x} d\zeta \end{aligned} \quad (2.10)$$

Substituting (2.9) into (2.10), and rearranging the expression, we obtain

$$\begin{aligned} j \frac{\mu_2}{\mu_1} (b_n \sin \xi_n d + c_n \cos \xi_n d) \xi_n a \\ = \frac{a_n}{2\pi} \sum_{m=1}^{\infty} a_m (b_m \cos \xi_m d - c_m \sin \xi_m d) I(k_2) \end{aligned} \quad (2.11)$$

where

$$\begin{aligned} I(k_2) &= \int_{-\infty}^{\infty} \frac{[(-1)^m e^{j\zeta a} - e^{-j\zeta a}] [(-1)^n e^{-j\zeta a} - e^{j\zeta a}] k'_2}{(\zeta^2 - a_m^2)(\zeta^2 - a_n^2)} d\zeta \\ &= \frac{2\pi a \chi_m}{a_m^2} \delta_{mn} - [I_1(k_2) + I_2(k_2)] \end{aligned} \quad (2.12)$$

where δ_{mn} is the Kronecker delta, and $\chi_m = \sqrt{k_2^2 - a_m^2}$. Substituting (2.6) into (2.5) and (2.12) into (2.11), we obtain the simultaneous equation for c_m and b_m which may be rewritten as the following matrix form:

$$\begin{bmatrix} \Psi_1 & \Psi_2 \\ \Psi_3 & \Psi_4 \end{bmatrix} \begin{bmatrix} B \\ C \end{bmatrix} = \begin{bmatrix} \Gamma \\ 0 \end{bmatrix}$$

where B and C are column vectors consisting of elements b_m and c_m , respectively, and $\Psi_1, \Psi_2, \Psi_3, \Psi_4$, and Γ are matrices whose elements are such as

$$\begin{aligned} \psi_{1,nm} &= \frac{ja\eta_n}{\mu_0} \delta_{mn} - \frac{ja_n}{2\pi\mu_0} a_m [I_1(k_0) + I_2(k_0)] \\ &\equiv \psi_1^{(0)} \delta_{mn} + \psi_1^{(1)} \\ \psi_{2,nm} &= -\frac{a\xi_n}{\mu_1} \delta_{mn} \\ &\equiv \psi_2^{(0)} \delta_{mn} \end{aligned}$$

$$\begin{aligned}
\psi_{3,nm} &= a \left(\frac{\chi_n}{\mu_2} \cos \xi_n d + \frac{\xi_n}{j\mu_1} \sin \xi_n d \right) \delta_{nm} \\
&\quad - \frac{a_n a_m}{2\pi\mu_2} \cos(\xi_m d) [I_1(k_2) + I_2(k_2)] \\
&\equiv \psi_3^{(0)} \delta_{nm} + \psi_3^{(1)} \\
\psi_{4,nm} &= a \left(-\frac{\chi_n}{\mu_2} \sin \xi_n d + \frac{\xi_n}{j\mu_1} \cos \xi_m d \right) \delta_{nm} \\
&\quad + \frac{a_n a_m}{2\pi\mu_2} \sin(\xi_m d) [I_1(k_2) + I_2(k_2)] \\
&\equiv \psi_4^{(0)} \delta_{nm} + \psi_4^{(1)} \\
\gamma_n &= \frac{2jk_z a_n}{\mu_0(a_n^2 - k_z^2)} [-(-1)^n e^{jk_z a} + e^{-jk_z a}]
\end{aligned}$$

Solving the above matrix for B and C , we have

$$\begin{aligned}
B &= (\Psi_1 - \Psi_2 \Psi_4^{-1} \Psi_3)^{-1} \Gamma \\
C &= -\Psi_4^{-1} \Psi_3 (\Psi_1 - \Psi_2 \Psi_4^{-1} \Psi_3)^{-1} \Gamma
\end{aligned} \quad (2.13)$$

We consider the following two special cases:

i) When $d = 0$ and $k_0 = k_2$, then

$$\begin{aligned}
B &= \frac{1}{2} \Psi_1^{-1} \Gamma \\
C &= \frac{1}{2} \Psi_2^{-1} \Gamma
\end{aligned}$$

Furthermore if $k_0 a \ll 1$, then $b_1 \approx -j1.3k_z a$, $c_1 \approx -0.8k_z a$, and $b_n \approx c_n \approx 0 (n \neq 1)$

ii) When $k_0 a \gg 1$, then

$$\begin{aligned}
b_n &\approx \frac{\psi_4^{(0)} \gamma_n}{\psi_2^{(0)} \psi_3^{(0)} - \psi_1^{(0)} \psi_4^{(0)}} \\
c_n &\approx \frac{\psi_3^{(0)} \gamma_n}{\psi_2^{(0)} \psi_3^{(0)} - \psi_1^{(0)} \psi_4^{(0)}}
\end{aligned} \quad (2.14)$$

III. SCATTERED AND TRANSMITTED FIELD COMPUTATION

Substituting b_m and c_m given in the previous section into $\tilde{E}_y^s(\zeta)$ and $\tilde{E}_y^t(\zeta)$, we obtain the scattered and transmitted fields, $E_y^s(x, z)$ and $E_y^t(x, z)$. In order to check the validity of our formulation, we compared $|E_y^s(x, 0)|$ and $|E_y^t(x, -d)|$ of our computation with the magnetic currents given in Fig. 4(a) and (b) of [6], confirming perfect agreements between two results; hence, we do not show the comparison here.

The far-zone scattered and transmitted fields at distance r_1 and r_2 shown in Fig. 1 can be evaluated by utilizing the stationary phase approximation such as

$$\begin{aligned}
E_y^s(\theta_s, \theta) &= e^{j(k_0 r_1 - (\pi/4))} \sqrt{\frac{k_0}{2\pi r_1}} \cos \theta_s \\
&\quad \cdot \sum_{m=1}^{\infty} b_m a_m \frac{e^{-jk_0 a \sin \theta_s} (-1)^m - e^{jk_0 a \sin \theta_s}}{(k_0 \sin \theta_s)^2 - a_m^2} \\
E_y^t(\theta_t, \theta) &= e^{j(k_2 r_2 - (\pi/4))} \sqrt{\frac{k_2}{2\pi r_2}} \cos \theta_t \\
&\quad \cdot \sum_{m=1}^{\infty} [b_m \cos(\xi_m d) - c_m \sin(\xi_m d)] a_m \\
&\quad \cdot \frac{e^{-jk_2 a \sin \theta_t} (-1)^m - e^{jk_2 a \sin \theta_t}}{(k_2 \sin \theta_t)^2 - a_m^2}
\end{aligned}$$

where

$$\theta_s = \sin^{-1}(x/r_1), \quad r_1 = \sqrt{x^2 + z^2}$$

$$\theta_t = \sin^{-1}(x/r_2), \quad r_2 = \sqrt{x^2 + (z+d)^2}$$

In Fig. 2, we depict the angular behavior of the far-zone transmitted field, where (2.13; exact) and (2.14; approximate) are, respectively,

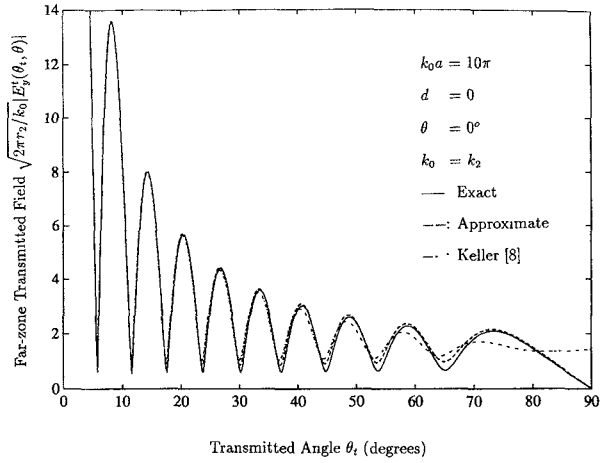


Fig. 2. Angular behavior of far-zone transmitted field.

used for b_n calculations. Fig. 2 shows that both exact and approximate solutions agree well with the Keller's high-frequency results [8] when $\theta_t < 60^\circ$.

The transmission coefficient, t , may be defined as a ratio of the time-averaged power transmitted through the slit to the time-averaged power incident on the slit, and the reflection coefficient, r , as a ratio of the scattered to the incident power. They are shown to be as

$$\begin{aligned}
t &\equiv \frac{\omega\mu_0}{2ak_0} \operatorname{Re} \left\{ \int_{-a}^a E_y^d(x, -d) H_x^{d*}(x, -d) dx \right\} \\
&= \operatorname{Im} \left\{ \frac{\mu_0}{2k_0\mu_1} \sum_{m=1}^{\infty} \xi_m^* [|b_m|^2 \cos \xi_m d (\sin \xi_m d)^* \right. \\
&\quad + b_m c_m^* | \cos \xi_m d |^2 - b_m^* c_m | \sin \xi_m d |^2 \\
&\quad \left. - |c_m|^2 \sin \xi_m d (\cos \xi_m d)^*] \right\} \\
r &\equiv \frac{\omega\mu_0}{2ak_0} \operatorname{Re} \left\{ \int_{-a}^a E_y^d(x, 0) H_x^{d*}(x, 0) dx \right\} \\
&= \frac{\mu_0 a}{2ak_0} \operatorname{Im} \left\{ \sum_{m=1}^{\infty} \frac{1}{\mu_1} b_m c_m^* \xi_m^* \right\}
\end{aligned} \quad (3.15)$$

where symbol $\operatorname{Im}\{\dots\}$ denotes taking an imaginary part of $\{\dots\}$ and symbol $(\dots)^*$ denotes a complex conjugate of (\dots) .

i) When $d = 0$ and $k_0 = k_2$, t and r simplify to

$$t = r = -\frac{\mu_0}{4ak_0} \operatorname{Im} \left\{ \sum_{m=1}^{\infty} b_m \gamma_m^* \right\}$$

ii) When $k_0 a \gg 1$, and $k_0 = k_1 = k_2$, we obtain approximate t and r in closed forms by substituting (2.14) into (3.15).

$$\begin{aligned}
t &\approx r \approx \frac{\mu_0^2}{8a^2 k_0} \sum_m \frac{|\gamma_m|^2}{\xi_m} \\
\text{where } 1 \leq m &< 2k_0 a / \pi,
\end{aligned} \quad (3.16)$$

It is interesting to note that the approximate t and r are independent of d . Using (3.15), we evaluate t versus θ for $k_0 a = 5$ and $d/a = 0, 0.8, 1.6$ when $k_0 = k_1 = k_2$ in Table I. We observe that our computations agree well with the results in [3] when $d/a = 0, 0.8$, but an appreciable difference exists between ours and [3] when $d/a = 1.6$.

The approximate t (3.16) is tabulated against the exact t (3.15) in Table II when $k_0 a = 15$ and $d/a = 0, 0.8, 1.6$. Table II shows that approximate solution agrees well with the exact one except for near grazing angles ($\theta \geq 70^\circ$).

TABLE I
ANGULAR BEHAVIOR OF TRANSMISSION COEFFICIENT FOR $k_0 a = 5$

θ	$k_0 a = 5$					
	$d/a = 0$		$d/a = 0.8$		$d/a = 1.6$	
	Hongo[3]	(3.15)	Hongo[3]	(3.15)	Hongo[3]	(3.15)
0°	1.0502	1.0410	1.0287	1.0280	1.0673	1.0547
10°	0.9678	0.9694	0.9600	0.9593	0.9951	0.9707
20°	0.8945	0.8885	0.8774	0.8767	0.9059	0.8768
30°	0.8991	0.8919	0.8654	0.8649	0.8806	0.8901
40°	0.8398	0.8328	0.7895	0.7902	0.7810	0.8469
50°	0.6271	0.6228	0.5776	0.5795	0.5509	0.6399
60°	0.3589	0.3572	0.3248	0.3267	0.2981	0.3677
70°	0.1502	0.1499	0.1340	0.1351	0.1188	0.1538
80°	0.0350	0.0350	0.0309	0.0312	0.0267	0.0357

TABLE II
ANGULAR BEHAVIOR OF TRANSMISSION COEFFICIENT FOR $k_0 a = 15$

θ	$k_0 a = 15$			Approximate (3.16)	
	Exact (3.15)	$d/a = 0$	$d/a = 0.8$	$d/a = 1.6$	
		$d/a = 0$	$d/a = 0.8$	$d/a = 1.6$	Exact (3.16)
0°	0.9974	0.9992	1.0007	1.0022	1.0022
10°	0.9768	0.9769	0.9781	0.9822	0.9822
20°	0.9201	0.9158	0.9161	0.9249	0.9249
30°	0.8488	0.8399	0.8409	0.8475	0.8475
40°	0.7692	0.7667	0.7694	0.7693	0.7693
50°	0.6112	0.6014	0.6020	0.6139	0.6139
60°	0.5226	0.5055	0.5116	0.5021	0.5021
70°	0.2764	0.2263	0.2312	0.2187	0.2187
80°	0.0632	0.0434	0.0445	0.0415	0.0415

IV. CONCLUSION

The behavior of TM-wave scattering from a slit in a thick conducting screen is reexamined. A Fourier transform approach is used to obtain the scattered and transmitted fields in series forms. Approximate solutions for scattering and transmission is presented in closed forms which are valid for high-frequency scattering.

REFERENCES

- [1] S. C. Kashyap and M. A. K. Hamid, "Diffraction characteristics of a slit in a thick conducting screen," *IEEE Trans. Antennas and Propagat.*, vol. AP-19, no. 4, pp. 499-507, July 1971.
- [2] L. N. Litvenenko, S. L. Prosvirnin, and V. P. Shestopalov, "Diffraction of a planar, H-polarized electromagnetic wave on a slit in a metallic shield of finite thickness," *Radio Engineering and Electronics, Physics*, vol. 22, pp. 35-43, Mar. 1977.
- [3] K. Hongo and G. Ishii, "Diffraction of an electromagnetic plane wave by a thick slit," *IEEE Trans. Antennas Propagat.*, vol. AP-26, no. 3, pp. 494-499, May 1978.
- [4] D. T. Auckland and R. F. Harrington, "Electromagnetic transmission through a filled slit in a conducting plane of finite thickness, TE case," *IEEE Trans. Microwave Theory Tech.*, vol. MTT-26, no. 7, pp. 499-505, July 1978.
- [5] O. M. Mendez, M. Cadilhac, and R. Petit, "Diffraction of a two-dimensional electromagnetic beam wave by a thick slit pierced in a perfectly conducting screen," *J. Opt. Soc. Am.*, vol. 73, no. 3, pp. 328-331, Mar. 1983.
- [6] J. M. Jin and J. L. Volakis, "TM scattering by an inhomogeneously filled aperture in a thick conducting plane," *Proc. Inst. Elec. Eng.*, vol. 137, Pt. H, no. 3, pp. 153-159, June 1990.
- [7] T. Park, H. J. Eom, and K. Yoshitomi, "An analytic solution for transverse-magnetic scattering from a rectangular channel in a conducting plane," *J. Appl. Phys.*, vol. 73, no. 7, pp. 3571-3573, Apr. 1993.
- [8] J. B. Keller, "Diffraction by an aperture," *J. Applied Physics*, vol. 28, no. 4, pp. 426-444, Apr. 1957.